Title page

Word count: Abstract 250

Text 3442

Reference 2037

Total 5729

Table 1

Figures 4

Title

Trait, staging, and state markers of psychosis based on functional alteration of salience-related networks in the high-risk, first episode, and chronic stages

Authors

Jun Miyata, MD, PhD[1,4]; Toby Winton-Brown, MD, PhD[4]; Thomas Sedlak, MD, PhD[5]; Toshihiko Aso, MD, PhD[8]; Nicola Cascella, MD[5]; Jennifer Coughlin, MD[5]; Nicolas A. Crossley, MD, PhD[4,19]; Emrah Duezel, MD, PhD[31]; Takahiro Ezaki, PhD[26]; Masaki Fukunaga, PhD[17]; Carolyn Howell, MD[5]; Masanori Isobe, MD, PhD[1]; Kouhei Kamiya, MD, PhD[29]; Kiyoto Kasai, MD, PhD[25,28]; Takanori Kochiyama, PhD[10]; Shinsuke Koike, MD, PhD[23,24,27,28]; Akira Kunimatsu, MD, PhD[12]; Naoki Masuda, PhD[21,22]; Susumu Mori, PhD[6]; Yasuo Mori, MD, PhD[1]; Toshiya Murai, MD, PhD[1]; Kiyotaka Nemoto, MD, PhD[34]; Frederick Nucifora, PhD[5]; Kazutaka Ohi, MD, PhD[11,14]; Naohiro Okada, MD, PhD[25,28]; Yuki Sakai, MD, PhD[9]; Nobukatsu Sawamoto, MD, PhD[2]; Tsutomu Takahashi, MD, PhD[32,33]; Shinichi Urayama, PhD[3]; Yoshiyuki Watanabe, MD, PhD[20]; Crystal C. Watkins, MD, PhD[5]; Hidenaga Yamamori,

MD, PhD[13,16,18]; Yuka Yasuda, MD, PhD[15,16]; Ryota Hashimoto, MD, PhD[16]; Hidehiko Takahashi, MD, PhD[1,30]; Akira Sawa, MD, PhD[5,7]; Philip McGuire, MD, PhD[4]

Affiliations

1 Department of Psychiatry, Graduate School of Medicine, 2 Department of Human Health Sciences, Graduate School of Medicine, 3 Human Brain Research Center, Graduate School of Medicine, Kyoto University, Kyoto, Japan

4 Department of Psychosis Studies, Institute of Psychiatry, Psychology & Neuroscience, King's College London, London, United Kingdom

5 Departments of Psychiatry, Neuroscience, Biomedical Engineering and Genetic Medicine, School of Medicine, 6 Department of Radiology, School of Medicine, 7 Department of Mental Health, Bloomberg School of Public Health, Johns Hopkins University, Baltimore, MD, United States

8 Laboratory for Brain Connectomics Imaging, RIKEN Center for Biosystems Dynamics Research, Kobe, Japan

9 Brain Information Communication Research Laboratory Group, Advanced Telecommunications Research Institutes International, Kyoto, Japan

10 Brain Activity Imaging Center, ATR-Promotions, Kyoto, Japan

11 Department of Psychiatry, Gifu University Graduate School of Medicine, Gifu, Japan

12 Department of Radiology, International University of Health and Welfare Mita Hospital, Tokyo, Japan

13 Japan Community Health Care Organization Osaka Hospital, Osaka, Japan

14 Department of General Internal Medicine, Kanazawa Medical University, Uchinada, Ishikawa, Japan

15 Medical Corporation Foster, Osaka, Japan

16 Department of Pathology of Mental Diseases, National Institute of Mental Health, National Center of Neurology and Psychiatry, Kodaira, Tokyo, Japan

17 Department of System Neuroscience, Division of Cerebral Integration, National Institute for Physiological Sciences, Okazaki, Japan

18 Department of Psychiatry, Osaka University Graduate School of Medicine, Suita, Osaka, Japan

19 Department of Psychiatry, Pontificia Universidad Catolica de Chile, Santiago, Chile

20 Department of Radiology, Shiga University of Medical Science, Shiga, Japan

21 Department of Mathematics, 22 Computational and Data-Enabled Science and Engineering Program, State University of New York at Buffalo, Buffalo, NY, United States

23 Center for Evolutionary Cognitive Sciences (ECS), Graduate School of Art and Sciences, 24 Center for Integrative Science of Human Behavior (CiSHuB), 25 Department of Neuropsychiatry, Graduate School of Medicine, 26 Division of Advanced Logistic Science, Research Center for Advanced Science and Technology, 27 Institute for Diversity & Adaptation of Human Mind (UTIDAHM), 28 The International Research Center for Neurointelligence (WPI-IRCN), Institutes for Advanced Study (UTIAS), The University of Tokyo, Tokyo, Japan

29 Department of Radiology, Toho University Omori Medical Center, Tokyo, Japan

30 Department of Psychiatry and Behavioral Sciences, Graduate School of Medical and Dental Sciences, Tokyo Medical and Dental University, Tokyo, Japan

31 Institute of Cognitive Neuroscience, University College London, London, United Kingdom

32 Department of Neuropsychiatry, Graduate School of Medicine and Pharmaceutical

Sciences, 33 Research Center for Idling Brain Science, University of Toyama, Toyama, Japan

34 Department of Psychiatry, Faculty of Medicine, University of Tsukuba, Ibaraki, Japan

Previous presentations

Parts of this paper were presented at the Japanese Society of Schizophrenia Research virtual annual meeting 2021, 9-10 April 2021, and the Schizophrenia International Research Society virtual annual meeting 2021, 17-21 April 2021.

Locations of work

1. Department of Psychiatry, Graduate School of Medicine, Kyoto University, Kyoto, Japan

2. Department of Psychosis Studies, Institute of Psychiatry, Psychology & Neuroscience, King's College London, London, United Kingdom

Corresponding author

Jun Miyata, MD, PhD

Department of Psychiatry, Graduate School of Medicine, Kyoto University

54 Shogoin-Kawaharacho, Sakyo-ku, Kyoto 606-8507, Japan

Tel: +81-75-751-3386

Fax: +81-75-751-3246

E-mail: miyata10@kuhp.kyoto-u.ac.jp

Key words: aberrant salience hypothesis, hippocampus, midbrain, salience network, striatum, thalamus

Abstract

Objective: Salience is a critical mechanism for survival in animals, the alteration of which is postulated to play key role in psychosis, including the hippocampus-midbrain-striatal and anterior cingulate cortex (ACC)-insular (salience network: SN) systems. However, how these two systems contribute to the psychosis traits, staging, and state is unknown.

Methods: Eight scanners at seven sites recruited 29 ultra-high-risk (UHR) individuals and 25 matched healthy controls (HC), 81 first-episode psychosis (FEP) patients and 109 HC, and 99 chronic psychosis (ChrP) patients and 145 HC. Resting-state functional MRI data which were intensively denoised and site effect-removed revealed the two systems as comprising five networks: the medial temporal lobe network (MTLN), midbrain-thalamic and striatal parts of the basal ganglia network (BGN-MbThal and BGN-Str), and ACC and insular parts of the SN (SN-ACC and SN-Ins). Group difference and correlation with positive symptom of network measures were performed in each psychosis stage.

Results: Connectivity within the BGN-MbThal was reduced in FEP compared to HC ($p<0.05$, family-wise-error [FWE] corrected). Connectivity within the SN-ACC was reduced in UHR ($p<0.05$, FWE) and in FEP and ChrP at liberal thresholds, with effect size of UHR>FEP>ChrP. FEP showed increased brain-state instability among the five networks, and positive correlation between positive symptom and connectivity within and between the MTLN. The correlation was stronger in unmedicated than medicated, and in affective than non-affective psychosis patients (all $p<0.05$, FWE).

Conclusions: Two salience-related systems were associated with psychosis traits, staging, and state. Refining these findings will lead to the development of clinically usable biomarkers.

Text

Introduction

The term salience is defined as the quality of being particularly noticeable or important (Oxford Dictionary https://www.lexico.com). For survival, animals need to quickly allocate their limited attentional resources to salient stimuli in the surrounding world. Previous animal studies showed that midbrain-striatal dopaminergic activity coded motivational (reward and avoidance) salience (1–3), while human functional magnetic resonance imaging (fMRI) studies also revealed that the striatum is responsive to stimulus salience (4–7).

Alteration of the midbrain-striatum is indicated in a wide range of psychiatric conditions such as psychosis (8), addiction (9), and depression (10). Psychosis is a broad term for severe mental disorders with delusions and/or hallucinations (i.e., positive symptoms (11)), the most common of which is schizophrenia. Elevated dopamine levels in the striatum of patients with schizophrenia (12) are hypothesized to cause aberrantly heightened salience attribution to ordinary stimuli, leading to delusions and hallucinations (aberrant salience hypothesis) (8). Additionally, recent circuit models of psychosis indicate that over-activity of glutamatergic neurons in the hippocampus triggers midbrain activation, leading to a hyperdopaminergic state in the striatum (13). These findings are consistent with recent studies of psychosis patients (14, 15). Thus, the hippocampus-midbrain-striatal system plays a critical role in aberrant salience in psychosis.

Human fMRI studies have described another neural system, the "salience network (SN)", which mainly comprises the anterior cingulate cortex (ACC) and bilateral insula, and which is activated by the salience of stimuli rather than the nature of tasks (16, 17). Studies have reported SN alterations in schizophrenia (18–20), obsessive-compulsive disorder (21), and autism spectrum disorder (22). However, a critical unanswered question is the role of the ACC-insular SN system in the aberrant salience of psychosis; in other words, how do these

two salience-related systems contribute to the pathophysiology of psychosis?

Resting-state fMRI (rsfMRI), fMRI scanning while at rest, is widely used to investigate the functional connectivity of brain networks in psychiatric disorders. Independent component analysis (ICA) is a common method used to analyze functional connectivity in rsfMRI. ICA can identify networks representing the hippocampus-midbrain-striatal system and the ACC-insular SN system; the bilateral hippocampus was identified within the medial temporal lobe network (MTLN (23), also known as the meso/paralimbic network (24)): the midbrain and striatum were identified as the basal ganglia network (BGN (25)): and the SN comprised the ACC and insula (16). Investigating the connectivity within and between these three networks can answer the questions raised above.

Developing objective biomarkers is necessary for psychosis diagnosis, prevention, and treatment. Biomarkers are generally categorized as 1) trait markers, which are present throughout the disease course and are not changed by treatment; 2) staging markers, which are prominent in certain disease stages; and 3) state markers, which reflect symptoms and change according to the treatment (26–29). Meanwhile, the course of psychosis can be divided into ultra-high risk (UHR), post-onset or first-episode psychosis (FEP), and chronic psychosis (ChrP) stages (30). It is unclear if aberrant salience is associated with psychosis trait, stage, or state.

Thus, we investigated how the two salience-related systems were associated with the aberrant salience of psychosis using ICA of rsfMRI. Specifically, we tested whether functional connectivity within and between the MTLN, BGN, and SN was associated with the diagnosis of psychosis and/or positive symptom severity at the UHR, FEP, and ChrP stages. To fully describe the connectivity profile, we investigated dynamic (31) (temporally varying) network measures as well a static (temporally constant) (32) measures. We also investigated the effects of antipsychotic medication and psychosis type (affective or non-affective) on connectivity measures, to clarify the meaning of our findings.

Methods

Participants

We recruited 1) 29 UHR individuals and 25 age-, sex-, and ethnicity-matched healthy controls (HC), 2) 81 FEP patients and 109 matched HC, and 3) 99 ChrP patients and 145 matched HC, comprising 488 subjects in total, from eight scanners at seven sites: the Institute of Psychiatry, Psychology, and Neuroscience (IoPPN), UK; Johns Hopkins University Hospital (JHU), USA; Kanazawa Medical University (KMU), Japan; Kyoto University (Kyoto), Japan; 2 MRI scanners of Osaka University (OSK), Japan; The University of Tokyo (Tokyo), Japan; and University of Toyama (TYM), Japan (Table 1). The details are described in the Supplemental Methods and Supplemental Tables 1-7 in the Supplemental Material. The Japanese sites were members of Cognitive Genetic Collaborative Research Organization (COCORO) consortium. Hereafter, we refer to UHR individuals as patients to refer to UHR, FEP and ChrP as a whole.

UHR was defined according to the Comprehensive Assessment of At-Risk Mental States (CAARMS) (33). FEP and ChrP were defined as duration of illness (DOI) of ≤ 36 and > 36 months, respectively. UHR individuals from IoPPN were unmedicated for antipsychotics, except for one patient (50mg quetiapine). JHU had both unmedicated (N=4) and medicated (N=47) FEP patients. All FEP and ChrP patients from KMU, OSK, and TYM were unmedicated. All FEP and ChrP patients from Kyoto and Tokyo were medicated. JHU had both affective (N=14, mood disorders with delusions/hallucinations) and non-affective (N=37, schizophrenia spectrum) psychosis patients. All the Japanese sites had non-affective psychosis patients only.

Symptomatology was assessed using CAARMS for UHR, and 1) the Scale for the Assessment of Positive Symptoms (SAPS) (34) and the Scale for the Assessment of Negative Symptoms (SANS) (35) or 2) the Positive and Negative Syndrome Scale (PANSS) (36) for FEP and ChrP at each site. The SAPS global summary score was converted to the PANSS positive score (37).

After receiving a complete description of the study, all participants provided written informed consent. The study design was approved by the institutional review boards of all sites:

Approved by Hammersmith Hospital Research Ethics Committee (IoPPN);

approved by Johns Hopkins Medicine Institutional Review Board (JHM IRB) (JHU);

approved by Research Ethical Committee of Kanazawa Medical University (KMU);

approved by Kyoto University Graduate School and Faculty of Medicine, Ethics Committee (Kyoto);

approval by Research Ethics Committee, Osaka University (OSK);

approved by Research Ethics Committee of the Faculty of Medicine of the University of Tokyo (Tokyo);

and approved by Ethics Committee, University of Toyama (TYM).

MRI acquisition and preprocessing

The rsfMRI and structural MRI data were acquired using 3-T MRI at each site. The details are provided in Supplemental Methods and Supplemental Table 8. Preprocessing procedure is described in Aso et al. (2017) (38) (ICA-based denoising criteria in the Supplemental Methods). Because the minimum number of volumes was 150 (Supplemental Table 8), we used 145 volumes for each site, discarding the first five volumes for signal stabilization. As an index of data quality, the temporal signal-to-noise ratio (tSNR) was calculated at each

voxel as the mean / SD of the time course and averaged for the whole brain using QAscript (39).

Meta-ICA

To identify the intrinsic networks, we performed meta-ICA (40, 41), which has higher robustness / reproducibility than conventional group ICA (gICA) (42). The meta-ICA comprised 2 steps:

First step: Preprocessed data of five patients (PT) and five HC were randomly selected from each site/scanner. Temporal concatenation gICA was then performed by the MELODIC (43) (version 3.15) toolbox of FSL (version 6.0.3) (http://www.fmrib.ox.ac.uk/fsl). This step was iterated 25 times (42).

Second step: a gICA was performed on the concatenation of 25 gICA results.

We repeated these steps, incrementing the total independent component (IC) number from 20 by 5. Networks of interest (NOIs: the MTLN, BGN, and SN) were clearly identified at IC = 80. The BGN was split into the midbrain-thalamus (BGN-MbThal) and striatum (BGN-Str) parts, while the SN was split into the ACC (SN-ACC) and the insula (SN-Ins) parts, for a total of five NOIs (Figure 1a).

Within-network analysis

Using dual regression (44) implemented in FSL, we first regressed each subject's preprocessed data against the meta-ICA maps created above to obtain subject-specific time courses for each IC. In the second step, we regressed the preprocessed data against the subject-specific time courses to obtain subject-specific spatial maps for each IC. The time courses of the five NOIs were selected for the statistical analysis.

Between-network analysis

We performed static between-network connectivity analysis, using the thresholded dual regression program (bug-fixed version) (45). After the second step of dual regression, mixture model thresholding was applied to each subject's spatial maps (43). We then regressed the preprocessed data against these thresholded maps to obtain subject-specific time courses that more accurately represented the network's time course compared to the first step of dual regression (45). Partial correlations between NOI-pairs were calculated using FSLNets version 0.6.3, running on MATLAB R2018b (MathWorks), while controlling for the effects of the other three NOIs. The correlation coefficients were Fisher-transformed into Z-scores.

Dynamic analysis

Next, we performed dynamic (31) analysis using the energy landscape analysis (ELA) (https://github.com/tkEzaki/energy-landscape-analysis) (46–51). Briefly, time courses of the five NOIs were binarized into "activated" and "deactivated" according to values above or below the mean. All subjects' data were concatenated and a pairwise maximum entropy model was fitted to the data, providing an "energy landscape" with two brain states (Figure 1b). State A had the local minima (frequent, low-energy pattern) with all five NOIs deactivated, while all NOIs were activated in state B. Finally, the frequency and transition rate of the brain states were calculated for each subject.

Harmonization

Difference between sites reportedly showed substantial effects in multi-site MRI studies (52–54). Thus, we estimated and removed additive and multiplicative site effects using an empirical Bayes framework with ComBat (55–57), from 1) each voxel of spatial maps of within-network analysis, 2) Z-transformed correlation coefficients of between-network analysis, and 3) frequency and transition rate of ELA.

Statistical analysis

Demographic and clinical data were analyzed using SPSS 27 for Windows (IBM). For all imaging analyses, permutation-based non-parametric inference was performed, using PALM (version 116) of FSL (58). In each stage, we performed 1) a group comparison and 2) multiple regression analysis with positive symptom severity, of the above network measures. Age, sex, and mean tSNR were used as covariates. Positive symptom severity was indexed by CAARMS "disorder of thought content" + "perceptual abnormalities" in UHR and PANSS positive score in FEP and ChrP. The statistical threshold was $p < 0.05$, correcting for multiple comparisons of:

A) Space (within-network analysis only): threshold-free cluster enhancement (TFCE) (59) within each NOI.

B) Number of contrasts: two contrasts (HC > PT and PT > HC, and positive or negative correlations).

C) Number of network/index: five NOIs for within-network analysis, 10 NOI-pairs for between-network analysis, and two indices (frequency and transition rate) for ELA.

We also reported more liberal thresholds of $p < 0.1$, corrected for space, contrast and network/index, and $p < 0.05$, corrected for space and contrast.

Effects of medication, psychosis type, and site

We investigated the effect of medication on significant group differences or correlations. In the case of within-network connectivity analysis, the mean value of the significant clusters was extracted. In the UHR group, we performed group comparisons or correlation analyses after excluding the patient administered 50mg quetiapine. In FEP and ChrP, we compared the network measures between unmedicated and medicated patients, and also investigated the interaction between medication and positive symptom severity on the network measures.

Age, sex, and tSNR were used as the covariates. The statistical threshold was set at $p < 0.05$, corrected for contrast, as well as for network/index if more than two networks/indices were found to be significant.

We examined the effect of psychosis type (affective and non-affective psychosis) as the same way.

To investigate the effect of site, we plotted the data and checked if the plots deviated according to the site/scanner. In addition, we supplementarily repeated the above analyses in only the JHU sample, which had both medication and psychosis types, to check whether the findings remained consistent.

Effects of smoking and substance use

We also similarly assessed the effect of smoking. Because some UHR and FEP patients had experience with substance use, we also investigated its effect.

Results

1) Demographic data

As shown in Table 1, there were no significant differences in age, sex, ethnicity, and mean tSNR between PT and HC in any stage. The number of years of completed education was lower in PT than in HC in all stages. Smoking and substance use were more prevalent in FEP than in HC.

2) Group comparisons

The within-network connectivity analysis showed significantly reduced connectivity within the BGN-MbThal in the right thalamus of FEP compared to HC ($p = 0.02$, corrected for

space, contrast, and network) (Figure 2a, middle row, left column). Connectivity within the SN-ACC was lower in UHR in the ACC than in HC ($p = 0.003$, corrected for space, contrast and network) (Figure 2a, top row, right column). Of note, the SN-ACC also showed reduced connectivity in FEP ($p = 0.07$, corrected for space, contrast, and network) and ChrP ($p = 0.08$, corrected for space and contrast) at almost the same locations as in UHR, at the liberal thresholds (Figure 2a, middle and bottom row respectively, right column). The effect sizes (Hedges' g) of the significant clusters for UHR, FEP, and ChrP were 1.45, 0.60, and 0.54, respectively. Other significant results at liberal thresholds are shown in the Supplementary Figure 1.

Between-network connectivity analysis revealed no significant difference in any stage, even at liberal thresholds.

The ELA revealed a significant increase in transition between brain states A and B for FEP compared to HC ($p = 0.003$, corrected for contrast and index) (Figure 2b). No other significant differences were observed, even at liberal thresholds.

3) Correlation with positive symptom

The within-network connectivity analysis showed a significant positive correlation between PANSS positive score and the MTLN in the left/right hippocampus and parahippocampal gyrus in FEP ($p = 0.03$ and $p = 0.02$ respectively, corrected for space, contrast and network) (Figure 3a). Supplementary Figure 2a also shows results at the liberal thresholds. No other significant correlations were observed.

The between-network connectivity analysis showed a significant positive correlation between PANSS positive score and connectivity between the MTLN and BGN-MbThal in

FEP ($p = 0.04$, corrected for contrast and network) (Figure 3b). Supplementary Figure 2b also shows significant results for liberal thresholds in the UHR and FEP. No other significant correlations were observed.

The ELA did not show significant correlations even at liberal thresholds.

4) Effect of medication, psychosis type, and site/scanner

None of the significant group comparison results above were affected by medication or psychosis type (Supplemental Results).

Analysis of the correlation of within-network connectivity revealed a significant interaction between medication type and PANSS positive score, with a steeper regression slope in unmedicated than in medicated patients (Figure 4a) ($p = 0.009$, corrected for contrast). We also observed significant interaction for psychosis type (Figure 4b), with a steeper slope in affective than in non-affective psychosis patients ($p = 0.003$, corrected for contrast). There was no clear deviation of plots according to the site/scanner (Figure 4c) and these interactions did not change when limited to the JHU sample.

Analysis of the correlation of between-network connectivity also showed significant interactions for medication and psychosis type (Figure 4d and 4e, $p = 0.01$ and 0.001, corrected for contrast, respectively), with steeper slopes in unmedicated and affective psychosis patients. There was no obvious deviation by site/scanner (Figure 4f) and the interactions did not change when limited to the JHU sample.

5) Effects of smoking and substance use

We observed no effect of smoking or substance use on any results of group comparison or correlation analysis (all $p > 0.05$, corrected).

Discussion

The main findings of this study were:

1: Reduced within-network connectivity and increased instability of two salience-related systems were observed in UHR and FEP compared to HC, with the SN showing significance levels and effect sizes in the order of UHR > FEP > ChrP.

2: Stronger connectivity within and between the hippocampus-midbrain-striatal system was associated with severer positive symptoms in FEP.

3: Finding 1 was not affected by medication or psychosis type, while finding 2 was attenuated in medicated and non-affective psychosis patients.

As a whole, we found fully corrected significance in UHR and FEP but not in ChrP, indicating that aberrant salience is more "salient" at early stages of psychosis (60). We discuss these findings further in the following sections.

Salience-related functional measures as trait/staging markers of psychosis

Regarding the hippocampus-midbrain-striatal system, we found reduced connectivity in the thalamus of the BGN in FEP. We recently reported heightened resting connectivity between the thalamus and cortical areas in FEP (61), in a sample that partially overlapped with the present study. Moreover, the thalamus was also recently reported to process salience (62). Our results have extended the knowledge of underlying structure of aberrant salience in psychosis. In contrast, we did not observe altered within-network connectivity in the striatum of the BGN in patients, while two previous ICA studies reported increased within-network connectivity (63, 64). Compared to these studies, we thoroughly considered confounding factors, as detailed in the Methods section, and strongly controlled for multiple comparisons.

For the ACC-insular SN system, we found reduced within-network connectivity, with

significance levels and effect sizes in the order of UHR > FEP > ChrP, in almost the same locations in the ACC (Figure 2a). This finding indicated that SN alteration is present throughout the stages and is weakened in later stages. These findings are also largely consistent with previous ICA studies, reporting reductions in the within-network connectivity of the SN in patients with schizophrenia (65–69).

This is the first ELA study to reveal frequent transitions between two brain states: that is, the increased instability of salience-related networks in FEP. Several previous studies reported increased instability between the SN, central executive network, and default mode network in schizophrenia, consistent with our findings (70, 71). The finding of synchronized fluctuation of all five NOIs in the two brain states is consistent with our view that the integration of different salience systems plays a key role in the pathophysiology of psychosis (72).

Importantly, the above findings were not affected by medication or psychosis type. Therefore, the within-network connectivity and brain-state transition of the two salience-related systems are candidate early-stage markers of psychosis; moreover, the ACC-insular SN system may also serve as a trait marker.

Hippocampus-midbrain-striatal functional connectivity as a state-related marker of psychosis

We observed an association between severer positive symptoms and stronger functional connectivity within the MTLN, and between the MTLN and BGN-MbThal in FEP. No other study has investigated the MTLN in psychosis using rsfMRI and ICA; thus, this finding is not only new also but important, as the hippocampus is postulated to be the starting point of dopaminergic aberrant salience in psychosis (13). The midbrain region of BGN-MbThal was also correlated with positive symptoms, although at a liberal threshold (Supplementary Figure

2a).

Importantly, these associations were attenuated in the medicated group, consistent with the requirement for state markers of psychosis (27, 28). We also found that this association was stronger in affective than in non-affective psychosis. As affective psychosis has better treatment responsiveness than non-affective psychosis (73), these findings may represent responsiveness to medication.

We did not observe association between positive symptoms and connectivity of the ACC-insular SN system at a fully corrected level, although we observed association at liberal thresholds (Supplementary Figure 2b). Taken together, these findings suggest that the functional connectivity of the hippocampus-midbrain-striatal system represents a state marker of aberrant salience, more than the ACC-insular SN system.

Robustness of the findings

The strengths of this study include the large sample size, intensive data denoising, robust estimation of the intrinsic networks by meta-ICA, accurate estimation of the network time course by thresholded dual regression (74–76), site-effect removal using ComBat, and intensive multiple comparison correction.

An unmedicated and affective FEP patient may appear to be an outlier in Figures 3 and 4, though Cook's distance (<0.5) indicated this was not true. Excluding this subject did not change the results except for the effect of psychosis type, potentially because of the small affective FEP sample size.

Limitations

First, owing to the difficulties in recruiting UHR populations and organizing multi-site studies, the UHR sample size was small compared to those of FEP and ChrP. Second,

medication and psychosis types were not perfectly balanced among sites, as described in the Methods section. However, harmonization effectively managed these differences. Third, we did not perform susceptibility-induced distortion correction because several sites did not have the field map necessary for this procedure. Fourth, a longitudinal study design would have been more suitable. However, to cover all stages, at least10 years of follow-up would be required, making such a design unrealistic. Finally, to develop clinically usable biomarkers, our findings require translation into more standardizable frameworks, such as multi-feature-based parcellation (77), and/or combining with other modalities (61, 78–80).

Conclusions

Functional alteration of the two salience-related systems, the hippocampus-midbrain-striatal system and ACC-insular SN system, were mainly associated with the early stages of psychosis. Alteration of the latter may also be a trait marker common to all stages, while the former was a state marker, reflecting both positive symptoms and antipsychotic treatment. Further refinement of these findings is necessary for precision psychiatry. Our focus on certain pathophysiological models/hypotheses (aberrant salience), identification of networks in a data-driven manner, and utilization state-of-the-art denoising and harmonization methods benefit research on salience-related disorders such as addiction, as well as a wide range of psychiatric disorders.

Authorship

JM had full access to all the data and takes responsibility for its integrity and the accuracy of the data analysis. JM, TWB, TM, HT, AS, and PM contributed to the study concept and design. All authors contributed to data acquisition, analysis, and interpretation. JM performed

the statistical analyses. JM drafted the manuscript. All authors contributed to the critical revision of the manuscript for important intellectual content.

Disclosures and acknowledgments

All authors declare that they have no conflicts of interest regarding the submission of this manuscript, related to financial support or relationships. The authors wish to extend their gratitude to the patients and volunteers for their participation in this study. They also thank all the lab and COCORO consortium members for their contributions and Editage (www.editage.com) for English language editing.

Grant support

This work was supported by JSPS/MEXT KAKENHI grants 26461767 (JM), 17H04248 (JM), 18H05130 (JM), 20H05064 (JM), 19H03583 (HT), 23120009 (HT), 16H06572 (HT), 20K21567 (HT), 15H04893 (TM), 16H06397 (TM), JP16H06280 (KK), JP18K07550 (TT), and JP21K12153 (KN); JST ImPACT grant 15808865 (TM) and Moonshot R&D grant JPMJMS2021 (SK and KK); grants from the Japan Foundation for Aging and Health (HT); AMED Strategic Research Program for Brain Sciences grants 17dm0107044h0005 (HT) and 20dm0107088h0005 (TM), Brain/MINDS & beyond studies 21dm0307008h0004 (JM, HT), 20dm0307102h0002 (TM), JP21dm0307001 (KK), JP21dm020769 (KK), JP21dm0307004 (SK and KK), and JP21dm0307002 (RH), Brain Mapping by Integrated Neurotechnologies for Disease Studies JP20dm0207069 (SK and KK), and grants JP21dk0307103 (RH) and JP21uk1024002 (RH); Intramural Research Grant (3-1) for Neurological and Psychiatric Disorders of NCNP (RH); Novartis Pharma Research Grant (JM); a grant from SENSHIN

Medical Research Foundation (JM, HT); a grant from SUZUKEN Memorial Foundation (JM); Tanabe-Mitsubishi Pharma Research Grant (JM); a grant from Uehara memorial foundation; Kyoto University Global Frontier Project for Young Professionals (JM); Takeda Science Foundation (JM and HT); Kobayashi Magobei Memorial Foundation (HT); Smoking Research Foundation (HT); the Kato Memorial Trust for Nambyo Research (TM); the National Institute of Mental Health (NIMH) grant numbers MH-094268 (AS), MH-092443 (AS), MH-105660 (AS), and the Silvio O. Conte Center funded by NIMH (AS); the National Institute of Health grant numbers P41EB015909 (SM) and R01NS084957 (SM); grants from Stanley (AS), S-R/RUSK (AS) and NARSAD (AS). Some of the participant recruitment supported by Tanabe Mitsubishi Pharm. Co. Ltd. (AS), and a Wellcome Trust fellowship grant WT087779MA (TWB).

References

1. Matsumoto M, Hikosaka O: Two types of dopamine neuron distinctly convey positive and negative motivational signals. Nature 2009; 459:837–841

2. Matsumoto M, Takada M: Distinct Representations of Cognitive and Motivational Signals in Midbrain Dopamine Neurons. Neuron 2013; 79:1011–1024

3. Menegas W, Akiti K, Amo R, et al.: Dopamine neurons projecting to the posterior striatum reinforce avoidance of threatening stimuli. Nat Neurosci 2018; 21:1421–1430

4. Zink CF, Pagnoni G, Martin-Skurski ME, et al.: Human Striatal Responses to Monetary Reward Depend On Saliency. Neuron 2004; 42:509–517

5. Zink CF, Pagnoni G, Chappelow J, et al.: Human striatal activation reflects degree of stimulus saliency. NeuroImage 2006; 29:977–983

6. Jensen J, Smith AJ, Willeit M, et al.: Separate brain regions code for salience vs. valence during reward prediction in humans. Hum Brain Mapp 2007; 28:294–302

7. Cooper JC, Knutson B: Valence and salience contribute to nucleus accumbens activation. NeuroImage 2008; 39:538–547

8. Kapur S: Psychosis as a State of Aberrant Salience: A Framework Linking Biology, Phenomenology, and Pharmacology in Schizophrenia. Am J Psychiatry 2003; 160:13–23

9. Nestler EJ: Is there a common molecular pathway for addiction? Nat Neurosci 2005; 8:1445–1449

10. Clark L, Chamberlain SR, Sahakian BJ: Neurocognitive Mechanisms in Depression: Implications for Treatment. Annu Rev Neurosci 2009; 32:57–74

11. Crow TJ: Positive and Negative Schizophrenic Symptoms and the Role of Dopamine. Br J Psychiatry 1980; 137:383–386

12. Fusar-Poli P, Meyer-Lindenberg A: Striatal Presynaptic Dopamine in Schizophrenia, Part II: Meta-Analysis of [18F/11C]-DOPA PET Studies. Schizophr Bull 2013; 39:33–42

13. Lodge DJ, Grace AA: Hippocampal dysregulation of dopamine system function and the pathophysiology of schizophrenia. Trends Pharmacol Sci 2011; 32:507–513

14. Winton-Brown T, Schmidt A, Roiser JP, et al.: Altered activation and connectivity in a hippocampal–basal ganglia–midbrain circuit during salience processing in subjects at ultra high risk for psychosis. Transl Psychiatry 2017; 7:e1245

15. Modinos G, Allen P, Zugman A, et al.: Neural Circuitry of Novelty Salience Processing in Psychosis Risk: Association With Clinical Outcome. Schizophr Bull 2020; 46:670–679

16. Seeley WW, Menon V, Schatzberg AF, et al.: Dissociable Intrinsic Connectivity Networks for Salience Processing and Executive Control. J Neurosci 2007; 27:2349–2356

17. Dosenbach NUF, Fair DA, Miezin FM, et al.: Distinct brain networks for adaptive and stable task control in humans. Proc Natl Acad Sci 2007; 104:11073–11078

18. White TP, Joseph V, Francis ST, et al.: Aberrant salience network (bilateral insula and anterior cingulate cortex) connectivity during information processing in schizophrenia. Schizophr Res 2010; 123:105–115

19. Palaniyappan L, Simmonite M, White TP, et al.: Neural Primacy of the Salience Processing System in Schizophrenia. Neuron 2013; 79:814–828

20. Dong D, Wang Y, Chang X, et al.: Dysfunction of Large-Scale Brain Networks in Schizophrenia: A Meta-analysis of Resting-State Functional Connectivity. Schizophr Bull 2018; 44:168–181

21. Posner J, Song I, Lee S, et al.: Increased functional connectivity between the default mode and salience networks in unmedicated adults with obsessive-compulsive disorder. Hum Brain Mapp 2017; 38:678–687

22. Uddin LQ, Supekar K, Lynch CJ, et al.: Salience Network–Based Classification and Prediction of Symptom Severity in Children With Autism. JAMA Psychiatry 2013; 70:869–879

23. Shirer WR, Ryali S, Rykhlevskaia E, et al.: Decoding Subject-Driven Cognitive States

with Whole-Brain Connectivity Patterns. Cereb Cortex 2012; 22:158–165

24. Meda SA, Gill A, Stevens MC, et al.: Differences in Resting-State Functional Magnetic Resonance Imaging Functional Network Connectivity Between Schizophrenia and Psychotic Bipolar Probands and Their Unaffected First-Degree Relatives. Biol Psychiatry 2012; 71:881–889

25. Robinson S, Basso G, Soldati N, et al.: A resting state network in the motor control circuit of the basal ganglia. BMC Neurosci 2009; 10:137

26. Ritsner MS, Gottesman II: Where Do We Stand in the Quest for Neuropsychiatric Biomarkers and Endophenotypes and What Next? [Internet], inRitsner MS, editorThe Handbook of Neuropsychiatric Biomarkers, Endophenotypes and Genes. Dordrecht, Springer Netherlands, 2009, pp 3–21.[cited 2020 Nov 19] Available from: http://link.springer.com/10.1007/978-1-4020-9464-4_1

27. Khoury R, Nasrallah HA: Inflammatory biomarkers in individuals at clinical high risk for psychosis (CHR-P): State or trait? Schizophr Res 2018; 199:31–38

28. Lema YY, Gamo NJ, Yang K, et al.: Trait and state biomarkers for psychiatric disorders: Importance of infrastructure to bridge the gap between basic and clinical research and industry. Psychiatry Clin Neurosci 2018; 72:482–489

29. National Institute of Mental Health Strategic Plan | 200846

30. Sheitman BB, Lieberman JA: The natural history and pathophysiology of treatment resistant schizophrenia. J Psychiatr Res 1998; 32:143–150

31. Hutchison RM, Womelsdorf T, Allen EA, et al.: Dynamic functional connectivity: Promise, issues, and interpretations. NeuroImage 2013; 80:360–378

32. Sakoğlu Ü, Pearlson GD, Kiehl KA, et al.: A method for evaluating dynamic functional network connectivity and task-modulation: application to schizophrenia. Magn Reson Mater Phys Biol Med 2010; 23:351–366

33. Yung AR, Yuen HP, McGorry PD, et al.: Mapping the onset of psychosis: the Comprehensive Assessment of At-Risk Mental States. Aust N Z J Psychiatry 2005; 39:964–971

34. Andreasen NC: Scale for the assessment of positive symptons: SAPS. University of Iowa, 1984

35. Andreasen NC: Scale for the Assessment of Negative Symptoms. University of Iowa, 1981

36. Kay SR, Fiszbein A, Opler LA: The positive and negative syndrome scale (PANSS) for schizophrenia. Schizophr Bull 1987; 13:261–276

37. van Erp TGM, Preda A, Nguyen D, et al.: Converting positive and negative symptom scores between PANSS and SAPS/SANS. Schizophr Res 2014; 152:289–294

38. Aso T, Jiang G, Urayama S, et al.: A Resilient, Non-neuronal Source of the Spatiotemporal Lag Structure Detected by BOLD Signal-Based Blood Flow Tracking [Internet]. Front Neurosci 2017; 11[cited 2018 Mar 28] Available from: https://www.frontiersin.org/articles/10.3389/fnins.2017.00256/full

39. Roalf DR, Quarmley M, Elliott MA, et al.: The impact of quality assurance assessment on diffusion tensor imaging outcomes in a large-scale population-based cohort. NeuroImage 2016; 125:903–919

40. Smith SM, Fox PT, Miller KL, et al.: Correspondence of the brain's functional architecture during activation and rest. Proc Natl Acad Sci 2009; 106:13040–13045

41. Biswal BB, Mennes M, Zuo X-N, et al.: Toward discovery science of human brain function. Proc Natl Acad Sci 2010; 107:4734–4739

42. Poppe AB, Wisner K, Atluri G, et al.: Toward a neurometric foundation for probabilistic independent component analysis of fMRI data. Cogn Affect Behav Neurosci 2013; 13:641–659

43. Beckmann CF, Smith SM: Probabilistic independent component analysis for functional magnetic resonance imaging. IEEE Trans Med Imaging 2004; 23:137–152

44. Filippini N, MacIntosh BJ, Hough MG, et al.: Distinct patterns of brain activity in young carriers of the APOE-ε4 allele. Proc Natl Acad Sci 2009; 106:7209–7214

45. Bijsterbosch JD, Beckmann CF, Woolrich MW, et al.: The relationship between spatial

configuration and functional connectivity of brain regions revisited. eLife 2019; 8:e44890

46. Watanabe T, Hirose S, Wada H, et al.: A pairwise maximum entropy model accurately describes resting-state human brain networks. Nat Commun 2013; 4:1370

47. Watanabe T, Hirose S, Wada H, et al.: Energy landscapes of resting-state brain networks [Internet]. Front Neuroinformatics 2014; 8[cited 2018 May 9] Available from: https://www.frontiersin.org/articles/10.3389/fninf.2014.00012/full

48. Watanabe T, Masuda N, Megumi F, et al.: Energy landscape and dynamics of brain activity during human bistable perception. Nat Commun 2014; 5:4765

49. Ezaki T, Watanabe T, Ohzeki M, et al.: Energy landscape analysis of neuroimaging data. Phil Trans R Soc A 2017; 375:20160287

50. Watanabe T, Rees G: Brain network dynamics in high-functioning individuals with autism. Nat Commun 2017; 8:16048

51. Ezaki T, Sakaki M, Watanabe T, et al.: Age-related changes in the ease of dynamical transitions in human brain activity. Hum Brain Mapp 2018; 39:2673–2688

52. Yamashita A, Yahata N, Itahashi T, et al.: Harmonization of resting-state functional MRI data across multiple imaging sites via the separation of site differences into sampling bias and measurement bias. PLOS Biol 2019; 17:e3000042

53. Yoshihara Y, Lisi G, Yahata N, et al.: Overlapping but Asymmetrical Relationships Between Schizophrenia and Autism Revealed by Brain Connectivity. Schizophr Bull 2020; 46:1210–1218

54. Mori Y, Miyata J, Isobe M, et al.: Effect of phase-encoding direction on group analysis of resting-state functional magnetic resonance imaging. Psychiatry Clin Neurosci 2018; 72:683–691

55. Johnson WE, Li C, Rabinovic A: Adjusting batch effects in microarray expression data using empirical Bayes methods. Biostatistics 2007; 8:118–127

56. Fortin J-P, Parker D, Tunç B, et al.: Harmonization of multi-site diffusion tensor

imaging data. NeuroImage 2017; 161:149–170

57. Yu M, Linn KA, Cook PA, et al.: Statistical harmonization corrects site effects in functional connectivity measurements from multi-site fMRI data. Hum Brain Mapp 2018; 39:4213–4227

58. Winkler AM, Webster MA, Brooks JC, et al.: Non-parametric combination and related permutation tests for neuroimaging: NPC and Related Permutation Tests for Neuroimaging. Hum Brain Mapp 2016; 37:1486–1511

59. Smith SM, Nichols TE: Threshold-free cluster enhancement: Addressing problems of smoothing, threshold dependence and localisation in cluster inference. NeuroImage 2009; 44:83–98

60. Winton-Brown TT, Fusar-Poli P, Ungless MA, et al.: Dopaminergic basis of salience dysregulation in psychosis. Trends Neurosci 2014; 37:85–94

61. Faria AV, Zhao Y, Ye C, et al.: Multimodal MRI assessment for first episode psychosis: A major change in the thalamus and an efficient stratification of a subgroup. Hum Brain Mapp 2021; 42:1034–1053

62. Zhu Y, Nachtrab G, Keyes PC, et al.: Dynamic salience processing in paraventricular thalamus gates associative learning. Science 2018; 362:423–429

63. Sorg C, Manoliu A, Neufang S, et al.: Increased Intrinsic Brain Activity in the Striatum Reflects Symptom Dimensions in Schizophrenia. Schizophr Bull 2013; 39:387–395

64. Duan M, Chen X, He H, et al.: Altered basal ganglia network integration in schizophrenia. Front Hum Neurosci 2015; 561

65. Manoliu A, Riedl V, Doll A, et al.: Insular dysfunction reflects altered between-network connectivity and severity of negative symptoms in schizophrenia during psychotic remission. Front Hum Neurosci 2013; 7:216

66. Manoliu A, Riedl V, Zherdin A, et al.: Aberrant Dependence of Default Mode/Central Executive Network Interactions on Anterior Insular Salience Network Activity in Schizophrenia. Schizophr Bull 2014; 40:428–437

67. Wang Y, Tang W, Fan X, et al.: Resting-state functional connectivity changes within the default mode network and the salience network after antipsychotic treatment in early-phase schizophrenia. Neuropsychiatr Dis Treat 2017; Volume 13:397–406

68. Ohta M, Nakataki M, Takeda T, et al.: Structural equation modeling approach between salience network dysfunction, depressed mood, and subjective quality of life in schizophrenia: an ICA resting-state fMRI study [Internet]. Neuropsychiatr Dis Treat 2018; [cited 2018 Jul 5] Available from: https://www.dovepress.com/structural-equation-modeling-approach-between-salience-network-dysfunc-peer-reviewed-article-NDT

69. Orliac F, Naveau M, Joliot M, et al.: Links among resting-state default-mode network, salience network, and symptomatology in schizophrenia. Schizophr Res 2013; 148:74–80

70. Wang X, Zhang W, Sun Y, et al.: Aberrant intra-salience network dynamic functional connectivity impairs large-scale network interactions in schizophrenia. Neuropsychologia 2016; 93, Part A:262–270

71. Supekar K, Cai W, Krishnadas R, et al.: Dysregulated Brain Dynamics in a Triple-Network Saliency Model of Schizophrenia and Its Relation to Psychosis. Biol Psychiatry 2019; 85:60–69

72. Miyata J: Toward integrated understanding of salience in psychosis [Internet]. Neurobiol Dis 2019; [cited 2019 Mar 7] Available from: http://www.sciencedirect.com/science/article/pii/S0969996119300610

73. Demjaha A, Lappin JM, Stahl D, et al.: Antipsychotic treatment resistance in first-episode psychosis: prevalence, subtypes and predictors. Psychol Med 2017; 47:1981–1989

74. Harrison SJ, Woolrich MW, Robinson EC, et al.: Large-scale Probabilistic Functional Modes from resting state fMRI. NeuroImage 2015; 109:217–231

75. Bijsterbosch JD, Woolrich MW, Glasser MF, et al.: The relationship between spatial configuration and functional connectivity of brain regions. eLife 2018; 7:e32992

76. Mejia AF, Nebel MB, Wang Y, et al.: Template Independent Component Analysis: Targeted and Reliable Estimation of Subject-level Brain Networks using Big Data Population Priors. J Am Stat Assoc 2020; 115:1151–1177

77. Glasser MF, Coalson TS, Robinson EC, et al.: A multi-modal parcellation of human cerebral cortex. Nature 2016; 536:171–178

78. Wang AM, Pradhan S, Coughlin JM, et al.: Assessing Brain Metabolism With 7-T Proton Magnetic Resonance Spectroscopy in Patients With First-Episode Psychosis [Internet]. JAMA Psychiatry 2019; [cited 2019 Jan 10] Available from: https://jamanetwork.com/journals/jamapsychiatry/fullarticle/2719702

79. Kamath V, Lasutschinkow P, Ishizuka K, et al.: Olfactory Functioning in First-Episode Psychosis. Schizophr Bull 2018; 44:672–680

80. Faria AV, Crawford J, Ye C, et al.: Relationship between neuropsychological behavior and brain white matter in first-episode psychosis [Internet]. Schizophr Res 2019; [cited 2019 May 6] Available from: http://www.sciencedirect.com/science/article/pii/S0920996419301355

Table 1. Demographic and clinical characteristics of the participants.[a]

	UHR		FEP		ChrP		Total	
Site	HC	PT (Unmed)	HC	PT (Unmed)	HC	PT (Unmed)	HC	PT (Unmed)
IoPPN	25	29 (28)					25	29 (28)
JHU			73	51 (4)			73	51 (4)
KMU			6	4 (4)	9	4 (4)	15	8 (8)
Kyoto					41	46 (0)	41	46 (0)
OSK2			4	2 (2)	13	7 (7)	17	9 (9)
OSK3			11	7 (7)	24	14 (14)	35	21 (21)
Tokyo			10	14 (0)	53	26 (0)	63	40 (0)
TYM			5	3 (3)	5	2 (2)	10	5 (5)
Total	25	29 (28)	109	81 (20)	145	99 (27)	279	209 (75)
Age, mean (SD)	22.5 (2.5)	21.2 (3.1)	25.0 (4.5)	23.5 (6.4)	36.4 (10.1)	35.2 (10.5)		
Sex (F/M)	13/12	16/13	56/53	31/50	75/70	45/54		
Ethnicity (HC/PT)	Caucasian (12/14)		African (43/26)		Japanese			
	African & other (6/11)		Japanese (36/30)					
	Mixed (2/2)		Caucasian (26/19)					
	Unknown (5/2)		Other Asian (2/3)					
			Hispanic (0/1)					
			Mixed (1/1)					
			Unknown (1/1)					
Education (year)[b]	12.6 (0.9)	11.9 (1.2)*	15.0 (2.2)	13.2 (2.8)**	15.8 (2.3)	13.8 (2.4)**		
Smoking (Y/N)[c]	5/10	16/10	4/79	16/48*	11/78	13/52		

Substance (Y/N)[d]	0/25	4/25	2/107	11/67*	0/145	0/145
DOI (year)				1.2 (0.8)		12.2 (7.7)
CAARMS						
positive [e]		14.3 (6.8)				
total		51.1 (17.1)				
PANSS						
positive [f]				14.6 (4.9)		16.1 (5.2)
negative				16.3 (5.8)		18.1 (6.4)
general				37.3 (11.1)		34.1 (11.1)
CP eq [g]				315.7 (329.4)		451.4 (486.7)
Mean tSNR	1910.4 (387.9)	1956.9 (697.5)	7315.6 (5555.1)	8647.7 (6928.1)	11482.7 (8849.5)	9468.5 (8977.8)

* $p<0.05$
** $p<0.001$
a: No significant difference between HC and PT unless otherwise indicated.

b: Completed years of education was significantly shorter in UHR ($t=2.4$, $df=51$, $p=0.018$), FEP ($t=5.1$, $df=185$, $p<0.001$), and ChrP ($t=6.5$, $df=238$, $p<0.001$) PT compared to HCs.

c: Information about smoking was available only for IoPPN, JHU, Kyoto and Tokyo. There were more current smokers in FEP PT compared to HC (Chi-square=12.5, df=1, p=0.001 by Fisher's exact test).

d: Subjects from Japanese sites had no experience with substance use. There were more substance users in FEP PT compared to HC (Chi-square=10.6, df=1, p=0.002 by Fisher's exact test).

e: CAARMS positive scores were available for 26 UHR PT.

f: PANSS positive scores were available for 76 FEP and 94 ChrP PT.

g: One UHR subject was taking 50mg quetiapine. For FEP, calculated for 55 medicated patients with available dose information. For ChrP, calculated for all 72 medicated patients.

Abbreviations

CAARMS, Comprehensive Assessment of At-Risk Mental States; ChrP, chronic schizophrenia; CP eq, chlorpromazine equivalent; DOI, duration of illness; F, female; FEP, first-episode psychosis; HC, healthy control; UHR, high risk; IoPPN, Institute of Psychiatry, Psychology, and Neuroscience; JHU, Johns Hopkins University Hospital; KMU, Kanazawa Medical University; M, male; N, no; OSK2, scanner number 2 of Osaka University; OSK3, scanner number 3 of Osaka University; PANSS, positive and negative syndrome scale; PT, patients; Tokyo, The University of Tokyo; tSNR, temporal signal/noise ratio; TYM, Toyama University; Unmed, unmedicated; Y, yes.

Figure legends

Figure 1. Overall network findings

a) Five networks of interest (NOIs) from meta-ICA

Meta-ICA identified the hippocampus-midbrain-striatal system as the medial temporal lobe network (MTLN), the midbrain and thalamus part of the basal ganglia network (BGN-MbThal), and the striatal part of the BGN (BGN-Str). The analysis also identified the ACC (SN-ACC) and bilateral insular (SN-Ins) parts of the ACC-insular SN system. The results were thresholded at $P > 0.5$, using alternative hypothesis testing in a Gaussian/Gamma mixture model.

b) Energy landscape of the five NOIs

Energy landscape analysis classified $2^5 = 32$ "activity" patterns of five NOIs into two brain states: brain state A was characterized by the local minima where all five NOIs were deactivated (below the mean), while brain state B had the local minima of all five NOIs activated (above the mean). Yellow indicates high-energy, low-frequency patterns and blue indicates low-energy, high-frequency patterns.

Abbreviations

ACC, anterior cingulate cortex; ICA, independent component analysis; SN, salience network.

Figure 2. Group comparison results

a) Reduced within-network connectivity of the BGN-MbThal in FEP and SN-ACC in UHR patients.

UHR (n=29) patients were compared to matched HC (n=25), FEP (n=81) with matched HC (n=109), and ChrP (n= 99) with matched HC (n=145). Yellow and *** indicate a significant reduction of connectivity in patients at $p < 0.05$, corrected for space (threshold-free cluster

enhancement), two contrasts, and five NOIs. Orange and ** indicate trend-level significance at $p < 0.1$, corrected for space, contrast and NOI. Red and * indicate significance at $p < 0.05$, corrected for space and contrast. Note that significance of the SN-ACC was UHR > FEP > ChrP, as well as Hedge's g (1.45, 0.60, and 0.54 respectively). Light blue indicates the NOIs.

b) Increased transition between brain states in FEP (n=81) compared to HC (n=109)

Statistical threshold was at $p < 0.05$, corrected for two contrasts and two indices. Brain state A was characterized by the local minima where all five networks of interest (NOIs) were deactivated (below the mean), while brain state B had the local minima of all five NOIs activated (above the mean).

Abbreviations

ACC, anterior cingulate cortex; BGN, basal ganglia network; ChrP, chronic schizophrenia; FEP, first-episode psychosis; HC, healthy controls; UHR, high risk; Ins, insula; MbThal, midbrain and thalamus; MTLN, medial temporal lobe network; NOI, network of interest; SN, salience network; Str, striatum.

Figure 3. Correlational analysis results.

a) Positive correlation between PANSS positive scale and connectivity within the MTLN in FEP (n=76).

Yellow and *** indicate significance at $p < 0.05$, corrected for space by threshold-free cluster enhancement, two contrasts, and five NOIs. Orange indicates trend-level significance at $p < 0.1$, corrected for space, contrast and NOI. Light blue indicates the NOI.

b) Positive correlation between PANSS positive scale and static connectivity between the MTLN and BGN-MbThal in FEP (n=76).

*** indicates significance at $p < 0.05$, corrected for two contrasts and 10 NOI-pairs.

Abbreviations

ACC, anterior cingulate cortex; BGN, basal ganglia network; FEP, first-episode psychosis; UHR, high risk; Ins, insula; MbThal, midbrain and thalamus; MTLN, medial temporal lobe network; NOI, network of interest; PANSS, positive and negative syndrome scale; SN, salience network; Str, striatum.

Figure 4. Effects of medication, psychosis type, and site.

a) Interaction between medication type and PANSS positive score on the connectivity within the MTLN in FEP (n=76). Regression slope was steeper in unmedicated (n=20) than in medicated (n=56) FEP patients. Significance at $p < 0.05$, corrected for contrast.

b) Interaction between psychosis type and PANSS positive score on the connectivity within the MTLN in FEP (n=76). Regression slope was steeper in affective (n=13) than in non-affective (n=63) FEP patients. Significance at $p < 0.05$, corrected for contrast.

c) Plot of correlation by site. No clear site-derived deviation of correlation between PANSS positive score and within-network connectivity.

d) Interaction between medication type and PANSS positive score on the static connectivity between the MTLN and BGN-MbThal in FEP (n=76). Regression slope was steeper in unmedicated (n=20) than in medicated (n=56) FEP patients. Significance at $p < 0.05$, corrected for contrast.

e) Interaction between psychosis type and PANSS positive score on the static connectivity between the MTLN and BGN-MbThal in FEP (n=76). Regression slope was steeper in affective (n=13) than in non-affective (n=63) FEP. Significance at $p < 0.05$, corrected for contrast.

f) Plot of correlation by site. No clear site-derived deviation of correlation between PANSS

positive score and static-between network connectivity.

Abbreviations

BGN-MbThal, midbrain and thalamus part of the basal ganglia network; FEP, first-episode psychosis; JHU, Johns Hopkins University; KMU, Kanazawa Medical University; MTLN, medial temporal lobe network; OSK2, Osaka University MRI2; OSK3, Osaka University MRI3; PANSS, positive and negative syndrome scale; Tokyo, The University of Tokyo; TYM, University of Toyama.

a)

Hippocampus-midbrain-striatal system

ACC-insular SN system

MTLN

BGN

SN

MTLN

BGN-MbThal

BGN-Str

SN-ACC

SN-Ins

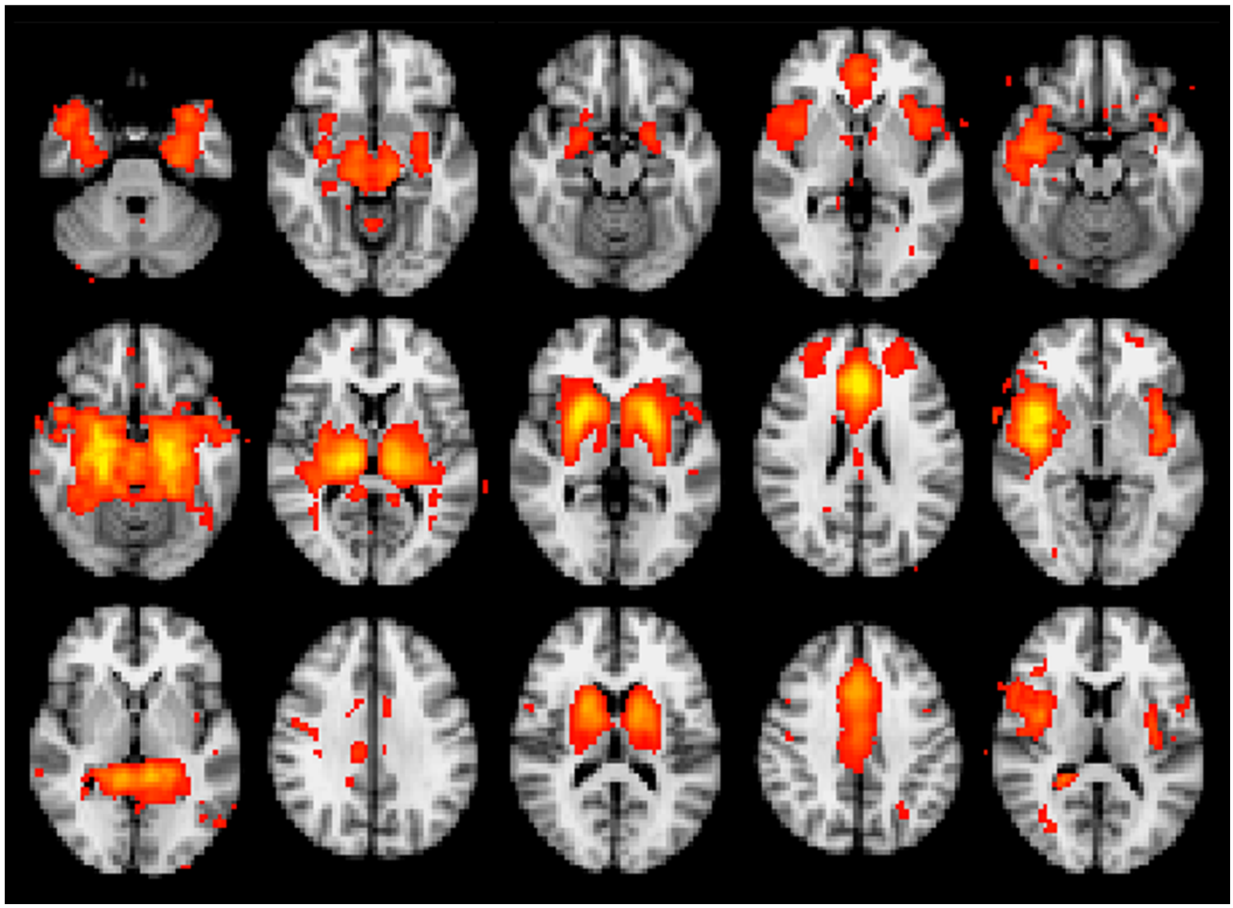

b)

Two-dimensional representation

Three-dimensional representation

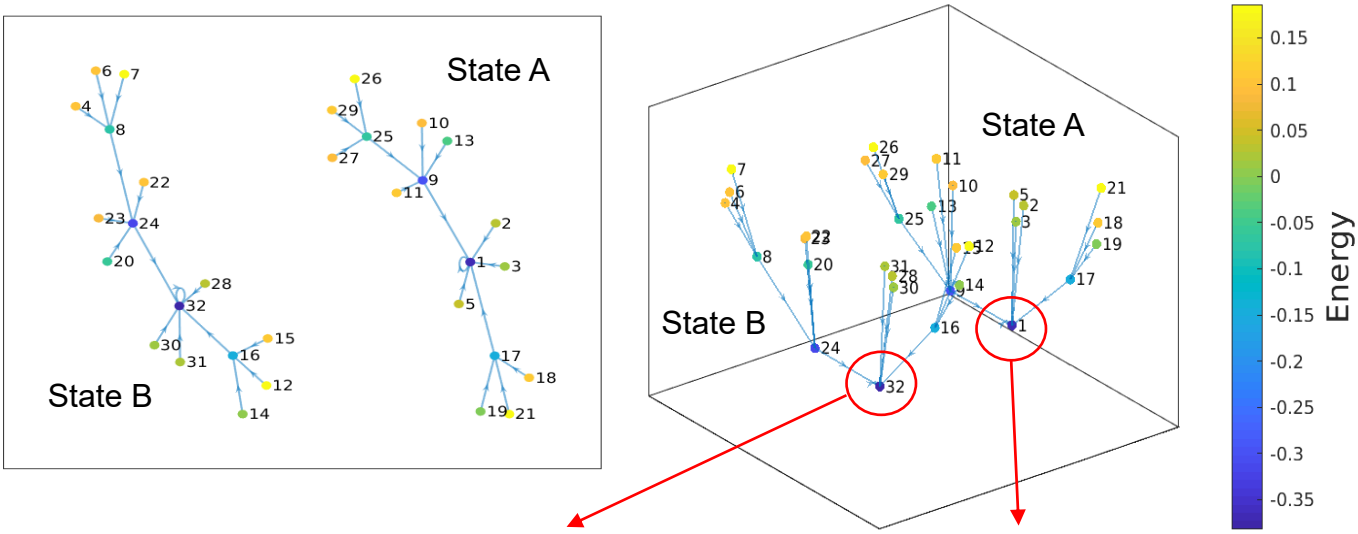

All five NOIs activated

All five NOIs deactivated

a)

HC > UHR

HC > FEP

HC > ChrP

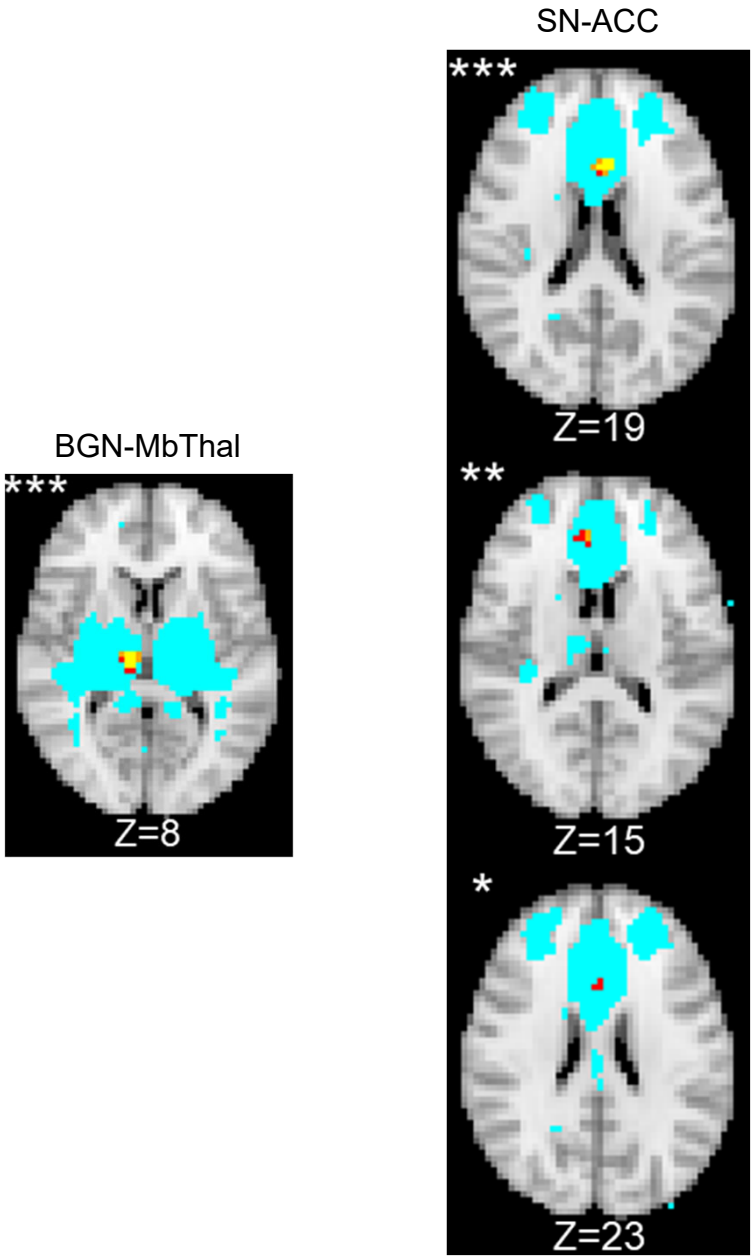

b)

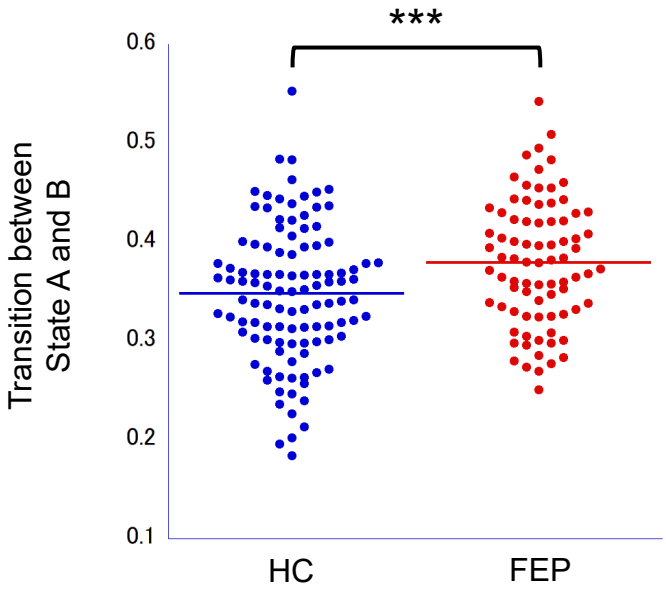

a)

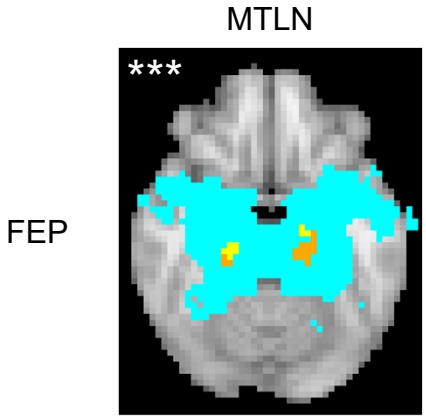
MTLN
***
FEP

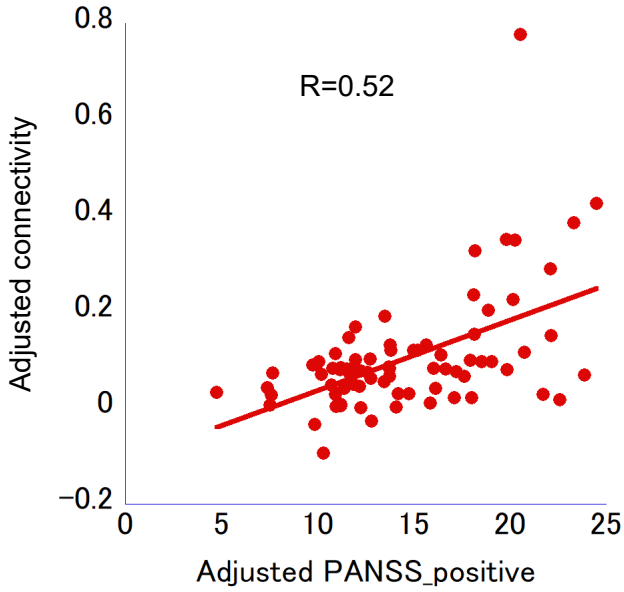
R=0.52
Adjusted connectivity
0.8
0.6
0.4
0.2
0
−0.2
0
5
10
15
20
25
Adjusted PANSS_positive

b)

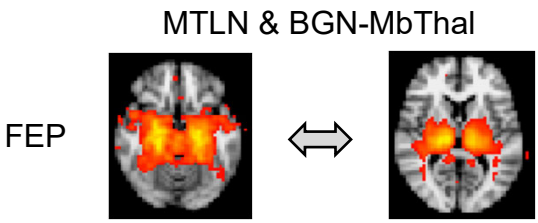
MTLN & BGN-MbThal
FEP

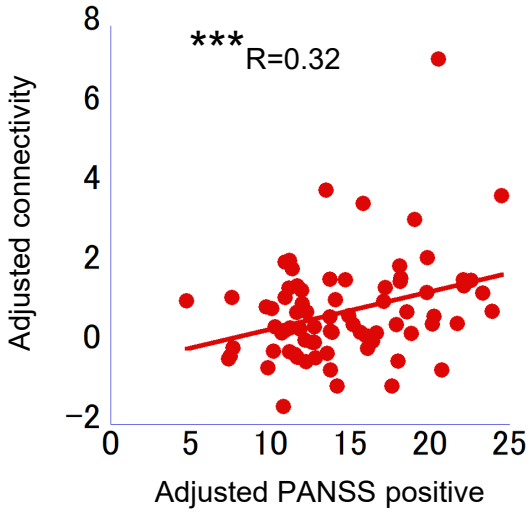
***
R=0.32
Adjusted connectivity
8
6
4
2
0
−2
0
5
10
15
20
25
Adjusted PANSS positive

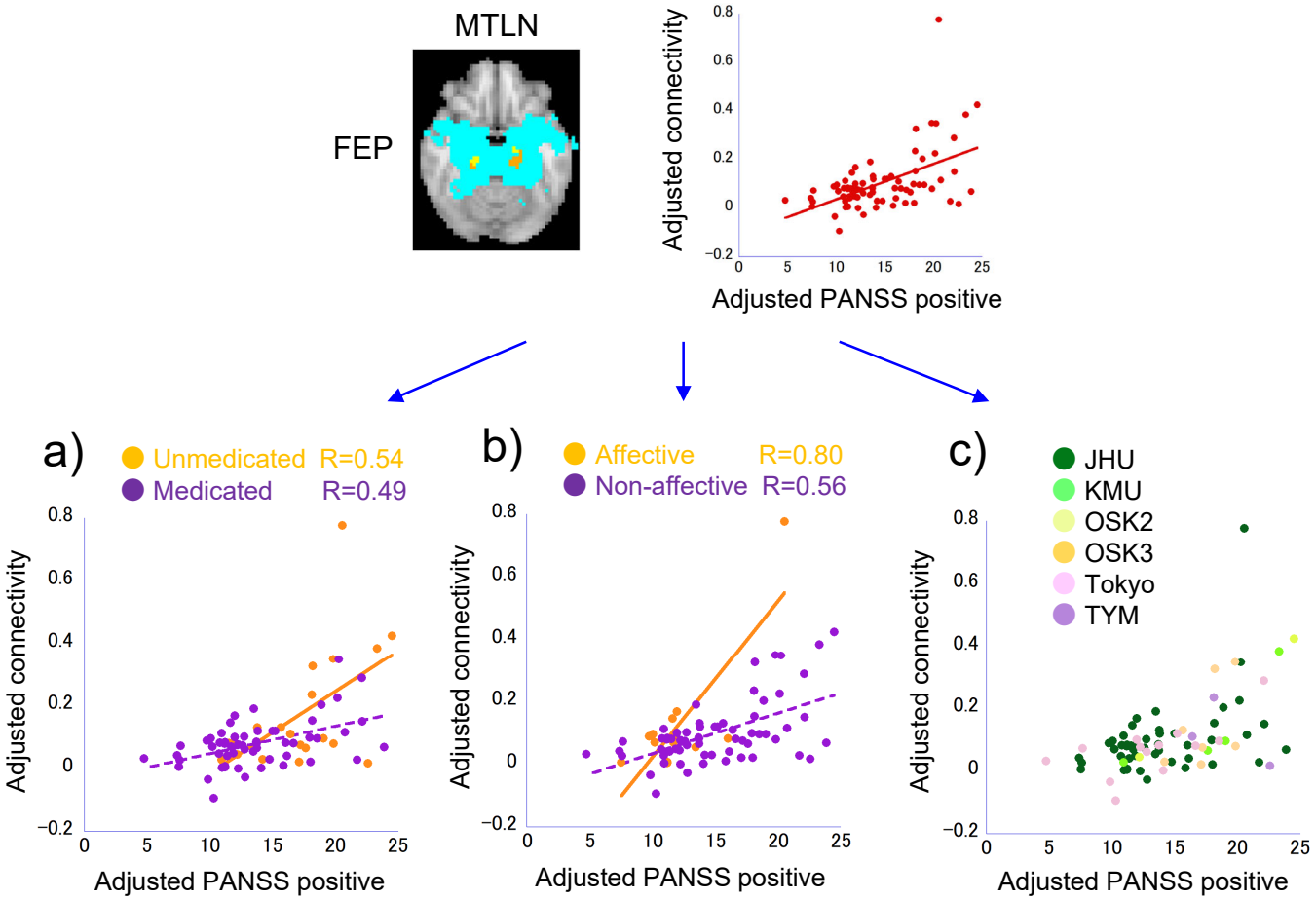
MTLN
FEP
Adjusted connectivity
Adjusted PANSS positive
a)
Unmedicated R=0.54
Medicated R=0.49
b)
Affective R=0.80
Non-affective R=0.56
c)
JHU
KMU
OSK2
OSK3
Tokyo
TYM

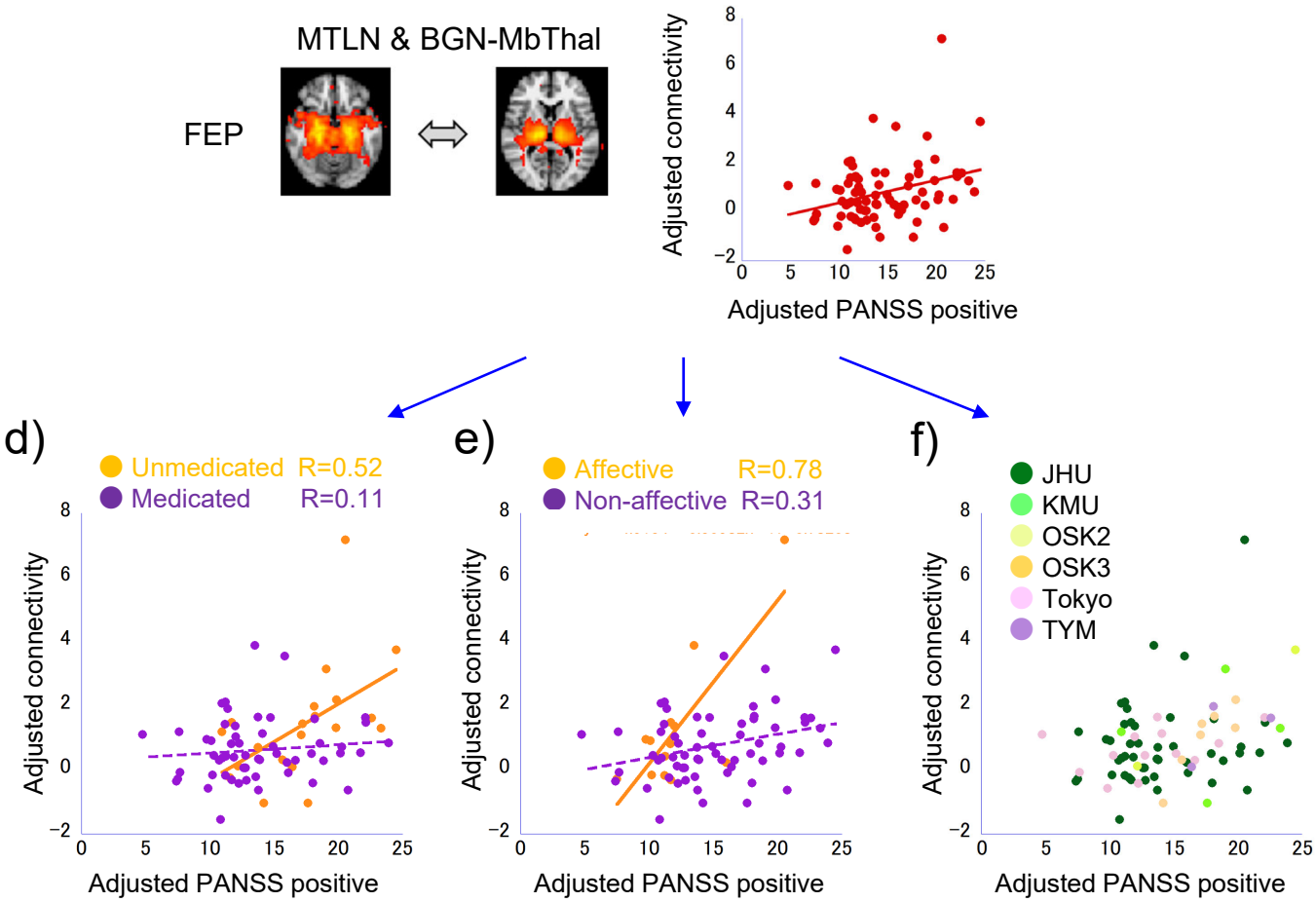
MTLN & BGN-MbThal
FEP
Adjusted connectivity
Adjusted PANSS positive
d)
Unmedicated R=0.52
Medicated R=0.11
e)
Affective R=0.78
Non-affective R=0.31
f)
JHU
KMU
OSK2
OSK3
Tokyo
TYM